Study of Dimming and LED Nonlinearity for ACO-OFDM Based VLC Systems

Irina Stefan*, Hany Elgala* and Harald Haas *§
*Jacobs University Bremen, Campus Ring 1, 28759 Bremen, Germany, Email: i.stefan & h.elgala@jacobs-university.de
§Institute for Digital Communications, The University of Edinburgh, Edinburgh EH9 3JL, UK, Email: h.haas@ed.ac.uk

***Abstract*—In this paper, the performance of an asymmetrically clipped optical orthogonal frequency division multiplexing (ACO-OFDM) indoor wireless system is investigated. In particular, the illuminance distribution inside a room (5 m×5 m×3 m) under different brightness conditions, *i.e.* dimming levels, and the electrical signal-to-noise ratio (SNR) at the receiver are considered. The system performance is also assessed in terms of bit-error-ratio (BER) as a function of average transmitted optical power. Brightness control is achieved using the continuous current reduction (CCR) technique to assure higher luminous efficacy compared to the pulse-width modulation (PWM) dimming technique. In addition, the impact of the induced distortions due to the nonlinear behavior of the light-emitting diode (LED) as a light source is included in the simulation model. For a circular area of about 1 m radius located directly below one of the four LED illumination modules utilized in the room, having illuminance values above 300 lx (10% brightness), a 9 dB average electrical SNR is achieved at the receiver located on a desktop.**

***Index Terms*—Optical wireless communication, OFDM, Nonlinearity, LED, dimming.**

I. Introduction

In recent years, interest in optical wireless (OW) as a promising complementary technology for radio frequency (RF) in short-range communications has gained new momentum. OW communications offer low energy consumption and high speed transmission for mobile communication infrastructures serving realtime bandwidth-intensive applications. Simple and low cost optical carrier modulation and demodulation are usually achieved through intensity modulation (IM) with direct detection (DD).

OFDM for OW systems is proposed to support high data rates through parallel transmission of high order multilevel quadrature amplitude modulation (M-QAM) symbols on orthogonal sub-carriers. In general, the output of the OFDM modulator is complex and bipolar. However, in IM optical systems, the baseband signal must be real and unipolar. Therefore, OFDM as commonly used in RF communications must be modified. The DC-biased optical OFDM (DCO-OFDM) and the ACO-OFDM are well known IM forms of optical OFDM [1–4]. In this paper, the ACO-OFDM is considered. In ACO-OFDM, the generated bipolar signal is converted to unipolar through clipping of all negative values at zero. ACO-OFDM requires less optical power for a given data rate than DCO-OFDM for all but the largest constellations, *e.g.* 1024-QAM. In addition, ACO is well suited to dimming systems, because it has better performance than DCO-OFDM at low SNR regime.

Dimming is an important attribute of light applications in order to be able to adjust illumination conditions in a room based on personal preferences and in order to safe energy. Two schemes are generally used for dimming LED, namely, continuous current reduction (CCR) and pulse-width modulation (PWM). In CCR, brightness control is achieved by decreasing the forward current while in the PWM scheme, the duty cycle of the forward current is changed. Reducing the forward current to realize dimming is a simple and cost effective way for dimming LEDs. The luminous intensity is reduced proportionally to the current and a brightness level of 10% of maximum is achievable. PWM is the preferred solution in industry for dimming LEDs because it offers a wide dimming range and a linear relationship between the light output and the duty cycle. The LED manufacturers also recommend PWM for dimming LEDs due to the general belief that LEDs exhibit low chromaticity shift under this dimming technique. In contrast, the experiments performed in [5, 6] show that the chromaticity shift for phosphor-converted (PC) white LEDs is small under both dimming schemes and that the luminous efficacy is always higher for the CCR dimming scheme, irrespective of the LED type. Moreover, a recent theoretical and experimental study [7] has shown that, contrary to the common adopted view, the CCR technique offers the best color stability over dimming due to the counteracting influences of drive current and junction temperature variations whereas an LED constantly suffers from non-eliminable chromaticity changes when PWM is used. It achieves this by properly selecting the heat sinks thermal resistance so that the overall chromaticity change is minimized. As a result the CCR is chosen as a dimming scheme for this study due to its simplicity and the benefits presented above. Induced distortion equations for ACO-OFDM due to the limited dynamic range of LEDs are derived in a closed form in [8]. These equations are used in this study to investigate the performance of an ACO-OFDM system in a practical room scenario where various lighting requirements (*e.g.* brightness levels) are viable.

The remainder of the paper is organized as follows: the ACO-OFDM system model and the LED nonlinearity effects are presented in Section II. In Section III, the simulation scenario inside a room is introduced. Simulation results including the illuminance and the SNR distributions as a function of the bias point and the transmitted optical power are discussed in Section IV. Finally, Section V concludes the paper.

978-1-4673-0437-5/12/$31.00 ©2012 IEEE

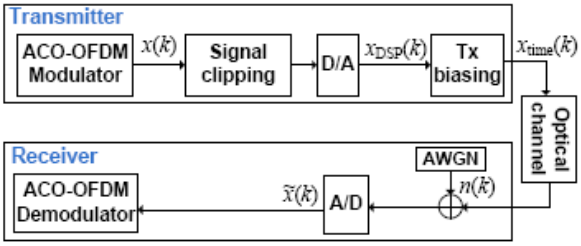

Fig. 1: OWC system based on the ACO-OFDM scheme. Signal clipping is realized in the digital domain.

II. ACO-OFDM SCHEME AND LED NONLINEARITY

In this paper, the ACO-OFDM scheme is considered. The optical transmission chain and the building blocks of the simulation model are briefly outlined in Fig. 1. The input stream of data-bits is first mapped into complex symbols according to the order of QAM modulation employed, *e.g.* 4-QAM. The IFFT operation is applied on the complex symbols to generate the ACO-OFDM modulating signal. For IM/DD systems, the signal modulating the LED intensity must be real-valued and positive. A real-valued ACO-OFDM signal is obtained by modulating only the odd sub-carriers (even sub-carriers are set to zero) and imposing a Hermitian symmetry on the input of the IFFT module. Signal clipping of all negative values converts the generated bipolar signal to unipolar. Thus, a real-valued positive ACO-OFDM signal in the time domain, $x(k)$ is obtained on the expense of 50% reduction in spectral efficiency in addition to the loss of spectral efficiency due to Hermitian symmetry. Additionally, the signal is limited due to the constraints imposed by the dynamic range of the LED.

The time domain ACO-OFDM signal, $x(k)$, follows a Gaussian distribution for IFFT sizes larger than 64 [9] due to the central limit theorem. Therefore, the average electrical symbol power is defined as: $E_{\text{s(elec)}} = 2\sigma^2_{x(k)}$ [8], where $\sigma^2_{x(k)}$ is the variance of $x(k)$. The forward current is the summation of the information carrying current, $x_{\text{DSP}}(k)$, and the forward bias current, X_{bias} (see Fig 2). The LED nonlinear transfer characteristic is compensated by predistorsion [10], which generates a linear characteristic only over a limited range. Due to the directly proportional relationship between the radiated optical power and the forward current through the LED, the signal and the constraints imposed by the transmitter front-end are described in terms of optical power. The limited dynamic range imposed by the LED is assumed between a point of minimum optical power, $P_{\text{Tx,min}}$ and a point of maximum optical power, $P_{\text{Tx,max}}$. The amount of optical power at the bias point is indicated by $P_{\text{Tx,bias}}$. Due to the maximum power driving limit of the LED, the signal is clipped at a top level, $\epsilon_{\text{top}} = P_{\text{Tx,max}} - P_{\text{Tx,bias}}$. If the LED is insufficiently forward biased, *i.e.* $P_{\text{Tx,bias}} < P_{\text{Tx,min}}$, the signal is additionally clipped at a bottom level, $\epsilon_{\text{bottom}} = P_{\text{Tx,min}} - P_{\text{Tx,bias}}$. The signal $x_{\text{DSP}}(k)$ obtained after the D/A conversion is used to modulate the intensity of the DC biased LED. The radiated optical signal, $x_{\text{time}}(k)$, is transmitted over a wireless channel characterized by a path loss coefficient, h.

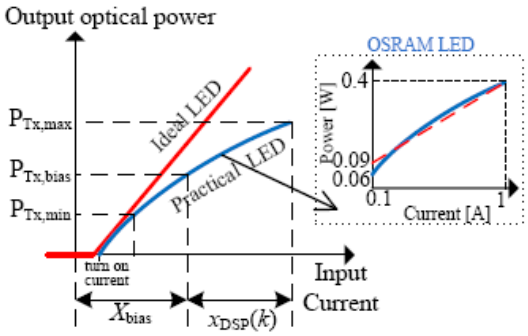

Fig. 2: LED transfer characteristic (optical power vs. forward current).

In order to characterize the nonlinear distortion caused by the physical range of the LED, the Bussgang theorem [9] is applied which states that the nonlinear distortion can be modeled as an attenuation of the transmitted signal plus a distortion noise component, $n_{\text{clip}}(k)$. As a result, the system performance is evaluated by introducing an effective SNR as the ratio between the power of the undistorted part of the signal and an effective noise power, which accounts for contributions caused by clipping as well as by shot and thermal noise $n(k)$:

$$\text{SNR}_{\text{eff}} = \frac{K^2 \left(E\left[x(k)\right]\right)^2}{\sigma^2_{\text{clip}} + \frac{\sigma^2_{n(k)}}{2h^2\gamma^2}} \tag{1}$$

where γ is the responsivity of the photodiode (PD) detector and $E\left[x(k)\right]$ is the useful signal power corresponding to the transmitted optical power in case of least signal clipping (*i.e.* $\lambda_{\text{bottom}} = 0$ and $\lambda_{\text{top}} = +\infty$) and neglecting the biasing power (see eq. (5) and eq. (6)). The variance of the white Gaussian noise, $\sigma^2_{n(k)}$, is the sum of the variance of the shot noise σ^2_{shot} and the thermal noise $\sigma^2_{\text{thermal}}$ and is given by:

$$\sigma^2_{n(k)} = \sigma^2_{\text{shot}} + \sigma^2_{\text{thermal}} \tag{2}$$

$$\sigma^2_{\text{shot}} = 2q\gamma P_r B + 2qI_{\text{bg}}B \tag{3}$$

$$\sigma^2_{\text{thermal}} = \frac{4kT}{R_L}B \tag{4}$$

where q is the electronic charge, I_{bg} is the background light noise current, B is the modulation bandwidth, P_r is the average optical received power, T is the absolute temperature, R_L is the load resistance and k is the Boltzmann's constant. The attenuation factor, K, and the variance of the clipping noise, σ^2_{clip}, are derived in [8] assuming a close to Gaussian distribution of the non-distorted signal. The clipping of an OFDM time domain signal results in a modification of its average optical power as follows [8]:

$$E\left[x_{\text{time}}(k)\right] = \sigma_{x(k)}\left(\phi(\lambda_{\text{bottom}}) - \phi\left(\lambda_{\text{top}}\right) + \lambda_{\text{top}}Q(\lambda_{\text{top}}) + \lambda_{\text{bottom}}Q(\lambda_{\text{top}})\right) + \max(P_{\text{Tx,min}}, P_{\text{Tx,bias}}) \tag{5}$$

where

$$\lambda_{\text{bottom}} = \frac{\epsilon_{\text{bottom}}}{\sigma_{x(k)}},\ \lambda_{\text{top}} = \frac{\epsilon_{\text{top}}}{\sigma_{x(k)}}, \tag{6}$$

$$\phi\left(u\right) = \frac{1}{\sqrt{2\pi}}\exp\left(-\frac{u^2}{2}\right), \tag{7}$$

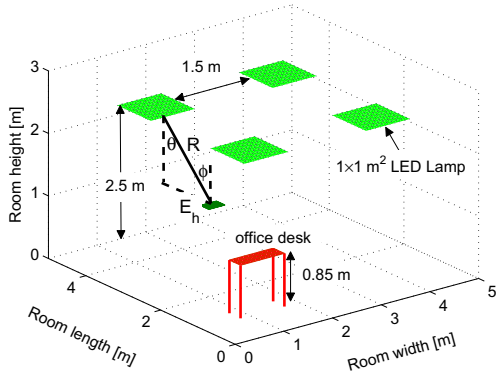

Fig. 3: Model room. Layout of ceiling lighting.

$$Q(u) = \frac{1}{\sqrt{2\pi}} \int_u^{\infty} \exp\left(-\frac{v^2}{2}\right) dv. \tag{8}$$

Here, $\phi(.)$ and $Q(.)$ are the respective probability mass function and complementary cumulative distribution function.

III. Simulation Scenario and System Parameters

The considered model with the exact dimensions and locations of the white-LEDs illumination modules is depicted in Fig. 3. The scenario in this paper is similar to the scenario described in [11]. Four illumination modules directed toward the floor provide the required illumination for the various office tasks and are placed at 0.5 m below the ceiling in a 5 m×5 m×3 m room. System performance is evaluated at desktop height (0.85 m above the floor) in a horizonal plane containing the user's optical receiver. Each illumination module has a dimension of 1 m×1 m and consists of 64 (8×8) high luminous intensity (27.3 cd) [12] white-LEDs, situated 14 cm apart. This scenario needs less than 300 LED chips compared to around 900 LED chips considered in [11]. The minimum illuminance for the working area (400 lx) according to the european lighting standard [13] is achieved at 15% brightness.

The illuminance is the most significant parameter when characterizing white-LEDs for illumination purposes. Assuming a Lambertian radiation pattern, the horizontal illuminance can be calculated as [11]:

$$\mathrm{E_h} = I_0 \cos^n(\theta) \cos\phi / R^2 \tag{9}$$

where ϕ is the angle of incidence, θ is the angle of irradiance, R is the distance to the illuminated surface (see Fig. 3), and I_0 is the maximal luminous intensity. The illuminance at any point of the receiving surface is evaluated by considering only the line-of-sight (LOS) signal path from each chip.

The channel DC gain from the i^{th} LED is given by [14]:

$$h_{\mathrm{LOS},i} \approx \frac{(n+1)A_R}{2\pi R_i^2} \cos^n(\theta_i) \cos(\phi_i) \mathrm{rect}(\theta_i/\mathrm{FOV}) \tag{10}$$

where A_R is the detector physical area, FOV is the receiver field of view, the lambertian index n depends on the viewing angle ($\theta_{1/2}$) of the LED as $n = -1/\log_2(\cos\theta_{1/2})$, and

$$\mathrm{rect}(x) = \begin{cases} 1 & \text{for } |x| \leq 1 \\ 0 & \text{for } |x| > 1 \end{cases} \tag{11}$$

TABLE I: Relevant parameters

LED characteristics	
Half intensity viewing angle, $\theta_{1/2}$	60°
Maximum luminous intensity, I_0	27.3 cd
Number of LED chips utilized in the room	256
Minimum emitted optical power, $P_{\mathrm{Tx,min}}$	90 mW
Maximum emitted optical power, $P_{\mathrm{Tx,max}}$	400 mW
Optical receiver characteristics	
Responsivity of SI based PD in the blue region, γ	0.28 A/W
Detector physical area, A_R	1 cm^2
Receiver field of view, FOV	85°
Background light noise current, I_{bg}	0.62 mA
Load resistance, R_L	10 kΩ
Absolute temperature, T	295°K

The light output characteristics for a practical LED are shown in Fig. 2. An OSRAM Golden Dragon white LED is considered in the simulations. The LED transfer characteristic (forward voltage vs forward current) is modeled through a sixth degree polynomial using the least-square curve fitting technique. Through predistortion [10], a linear response curve is achieved over a large range of the input signal amplitudes. However, the region which can be linearized is limited. For this type of LED the forward current varies from 100 mA to 1 A and the output optical power after the linearization procedure takes values from 90 mW to 400 mW. The model for an ideal LED is also depicted for comparison. For an ideal LED it is assumed that no saturation effect exists for infinite values of the driving current and that, the optical power emission is linearly proportional to the drive current. Below the turn on current no power is emitted. Table I, outlines the relevant simulation parameters.

IV. Simulation Results

The Monte Carlo simulation model realizes dimming through varying either the DC biasing optical power or the useful optical signal power. It is assumed that only upside clipping ($\lambda_{\mathrm{bottom}} = 0$) occurs due to the maximum power limit at the transmitter front-end, *i.e.* maximum allowed AC/pulsed current in the data-sheet. The LED is biased at a power level greater or equal to $P_{\mathrm{Tx,min}}$. It should also be noted that only the LOS signal path is considered.

Fig. 4 shows the achievable brightness in percentage as a function of transmitted optical power for the considered white LED. The transmitted optical power refers to the average optical power emitted by an LED chip, a sum of the signal power (including the nonlinear distorsion effects) and DC-bias point induced optical power (see eq. (5)). The lower limit is around 10% at 90 mW transmitted optical power, stemming from the predistorsion procedure which limits the LED dynamic range. A full brightness is considered at 0.4 W transmitted optical power. A second y-axis is also included to show the achievable dimming levels, which lie in the range from 0% to 72% for this type of LED. Dimming level of 0% (35% brightness) corresponds to the optical power of the recommended bias point in the datasheet (350 mA /180 mW).

Fig. 5 depicts the distribution of the illuminance at desktop

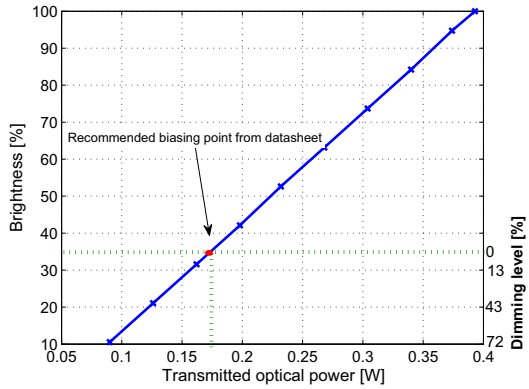

Fig. 4: Brightness versus transmitted optical power.

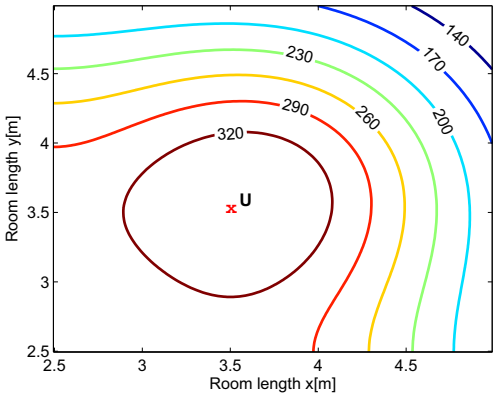

(a)

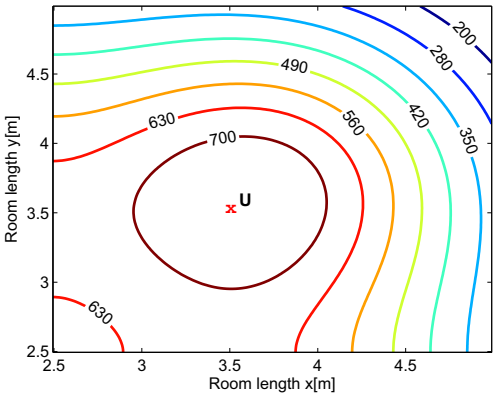

(b)

Fig. 5: The distribution of illuminance [lx] at (a) 10% brightness. (b) 35% brightness.

height for (a) 10% brightness (72% dimming) and (b) 35% brightness (0% dimming). Due to the geometric symmetry of the scenario, the illuminance distribution is plotted over a single quarter of the room. For 10% brightness the illumination is below 320 lx, appropriate when daylight is not sufficient and supplementary illumination is provided by LED light. For 35% brightness the illuminance is above 550 lx, for about 60% of the considered area which guarantees a well-lit office.

The performance is assessed in terms of average electrical SNR at the receiver calculated over an area with a radius of

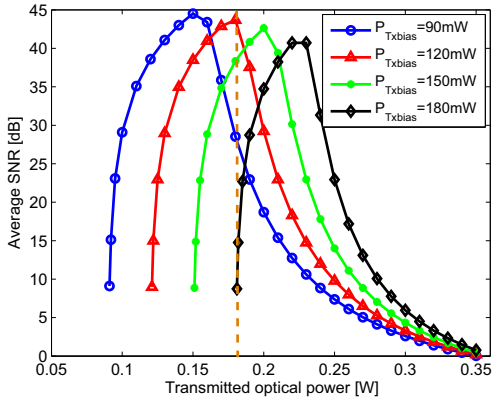

(a)

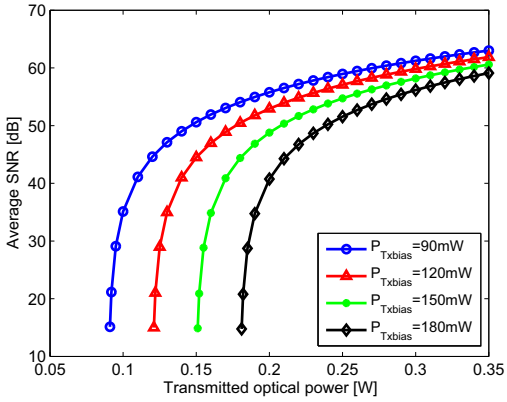

(b)

Fig. 6: The average electrical SNR versus the transmitted optical power for (a) a practical LED. (b) an ideal LED model.

1 m centered around the U-point (see Fig. 5). The obtained SNR values versus the transmitted optical power are shown in Fig. 6 (a) for different DC biasing optical power, $P_{\text{Tx,bias}}$. In Fig. 6 (b), the SNR values are plotted for an ideal LED, *i.e.* excluding the LED nonlinear behavior. A modulation bandwidth of 20 MHz is assumed. The SNR improves, as expected, with the increase of the useful optical signal power reaching an optimal value for a specific DC biasing optical power. By further increasing the useful optical signal power, the SNR starts to deteriorate as a result of induced nonlinear distortions caused by the LED limited dynamic range. Signal clipping is more pronounced in this case and the clipping noise becomes significant. An important observation is that by properly setting the biasing power, an optimum SNR is obtained for a wide range of brightness levels. For example at a brightness level of 35%, an optimum SNR, 44 dB, can be gained by setting the biasing power to 120 mW and the optical signal power to 60 mW, resulting in a total radiated power of 180 mW. The same brightness in the room is achieved at lower SNR, 38 dB, by selecting 150 mW biasing power in which case the optical signal power is 30 mW (180 mW total transmitted optical power). Or a worse choice leads to 29 dB SNR for a biasing power of 90 mW and optical signal power of 90 mW. At 15% brightness (400 lx), the SNR obtained is 37 dB, provided that the LED chip is biased at 90 mW and the

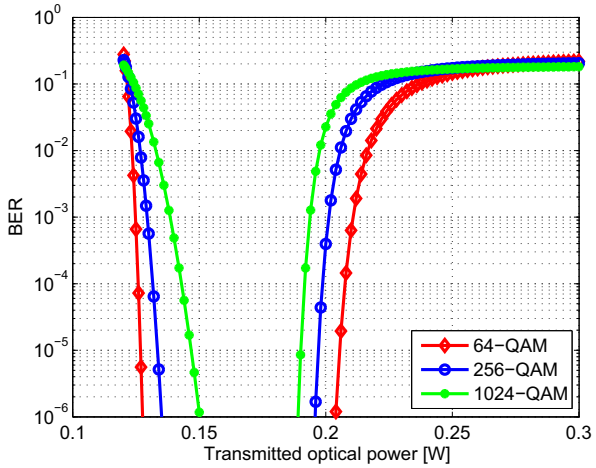

Fig. 7: The average BER versus the transmitted optical power for different modulation orders.

transmitted optical signal power is set to 25 mW, resulting in a transmitted optical power of 115 mW. At high transmitted optical power levels the maximum SNR that can be achieved is reduced even if high biasing power is applied. In this case the optical signal power is set relatively low to guarantee a specific brightness condition. These high transmitted optical power levels lead to illuminance values above 2000 lx which exceed the optimum levels for office lighting.

For the ideal LED, the SNR increases with an increase in the optical signal power, registering a saturation effect at high optical powers. When clipping is not included in the analysis, the most significant source of noise is the shot noise stemming from background radiation and received optical power.

The system performance can also be evaluated in a straightforward manner using the BER equations, i.e. for M-QAM, BER is evaluated using the expression [15]:

$$\text{BER} = \frac{4}{\log_2(M)}\left(1-\frac{1}{\sqrt{M}}\right) Q\left(\sqrt{\frac{3\text{SNR}_{\text{eff}}}{M-1}}\right) \qquad (12)$$

Fig. 7 depicts the BER performance for different QAM modulation orders as a function of the transmitted optical power. A 20 MHz bandwidth and a biasing power of 120 mW are assumed. The discontinuity in the BER curves indicate that the obtained BER is less than 10^{-7} for the corresponding transmitted optical powers. For low optical power levels (low SNR) the performance is noise dominant while clipping noise dominates at high optical power levels (greater than 0.23 W). For all curves it should be observed that there is a range of transmitted power levels where the performance is optimum. This range corresponds to the range of high SNR values in Fig. 6 (a) at 120 mW biasing power.

V. Conclusions

The performance of short-range indoor optical communication links based on ACO-OFDM as an energy efficient modulation scheme and commercial phosphors-based white-LEDs is investigated under various brightness/transmitted optical power levels. Signal power dependence of induced nonlinear effects clearly limits the maximum achievable data rates. The useful dimming range, to sustain an optical communication link, can be divided into different regions based on discrete bias point levels. The value of the transmitted optical power can be used to trigger the switch between the different regions. The DC optical power/bias point level must be changed adaptively to maximize the useful dimming range and to maintain a good SNR. It is also shown that AWGN noise dominates at low SNR values and clipping distortion dominates at large SNR values.

Acknowledgement

We gratefully acknowledge the support for this work from EADS Germany and Airbus Germany. In addition, we acknowledge the support from the German Federal Ministry of Economics and Technology (BMWi) under grant 20K0806G as part of the Lufo 2nd Call project SINTEG.

References

[1] Y. Tanaka, T. Komine, S. Haruyama, and M. Nakagawa, "Indoor Visible Light Data Transmission System Utilizing White LED Lights," *IEICE Transactions on Communications*, vol. E86-B, no. 8, pp. 2440–2454, Aug. 2003.

[2] H. Elgala, R. Mesleh, H. Haas, and B. Pricope, "OFDM Visible Light Wireless Communication Based on White LEDs," in *Proc. of the 64th IEEE Vehicular Technology Conference (VTC)*, Dublin, Ireland, Apr. 22–25, 2007.

[3] J. Armstrong and A. Lowery, "Power Efficient Optical OFDM," *Electronics Letters*, vol. 42, no. 6, pp. 370–372, Mar. 16, 2006.

[4] J. Armstrong and B. J. C. Schmidt, "Comparison of Asymmetrically Clipped Optical OFDM and DC-Biased Optical OFDM in AWGN," *IEEE Commun. Lett.*, vol. 12, no. 5, pp. 343–345, May 2008.

[5] Y. Gu, N. Narendran, T. Dong, and H. Wu, "Spectral and luminous efficacy change of high-power LEDs under different dimming methods," in *Proc. of SPIE 6337, 6th International Conference on Solid State Lighting*, San Diego, USA, 2006.

[6] M. Dyble, N. Narendran, A. Bierman, and T. Klein, "Impact of dimming white LEDs: Chromaticity shifts due to different dimming method," in *Proc. of SPIE 5941, 5th International Conference on Solid State Lighting*, Bellingham, WA, 2005, pp. 291–299.

[7] K. Loo, Y. Lai, S. Tan, and C. Tse, "On The Color Stability of Phosphor-Converted White LEDs Under DC, PWM, and Bi-Level Drive," *IEEE Transactions on Power Electronics*, vol. PP, no. 99, 2010.

[8] S. Dimitrov, S. Sinanovic, and H. Haas, "Double-sided Signal Clipping in ACO-OFDM Wireless Communication Systems," in *IEEE International Conference on Communications (IEEE ICC 2011)*, Kyoto, Japan, 5–9 Jun. 2011.

[9] D. Dardari, V. Tralli, and A. Vaccari, "A Theoretical Characterization of Nonlinear Distortion Effects in OFDM Systems," *IEEE Transactions on Communications*, vol. 48, no. 10, pp. 1755–1764, Oct. 2000.

[10] H. Elgala, R. Mesleh, and H. Haas, "Non-linearity effects and predistortion in optical OFDM wireless transmission using LEDs," *Inderscience Intenational Journal of Ultra Wideband Communications and Systems (IJUWBCS)*, vol. 1, no. 2, pp. 143–150, 2009.

[11] J. Grubor, S. Randel, K. Langer, and J. W. Walewski, "Broadband Information Broadcasting Using LED-Based Interior Lighting," *Journal of Lightwave Technology*, vol. 26, pp. 3883–3892, 2008.

[12] Osram Opto Semiconductors, "Datasheet: LCW W5SM Golden Dragon white LED," Retrieved from http://www.osram.de, Apr. 2011.

[13] European Standard EN 12464-1, "Lighting of Indoor Work Places," Jan. 2009.

[14] J. Barry, J. Kahn, W. Krause, E. Lee, and D. Messerschmitt, "Simulation of Multipath Impulse Response for Indoor Wireless Optical Channels," *IEEE J. Select. Areas Commun.*, vol. 11, no. 3, pp. 367–379, Apr. 1993.

[15] J. G. Proakis, *Digital Communications*, 4th ed., ser. McGraw-Hill Series in Electrical and Computer Engineering, S. W. Director, Ed. McGraw-Hill Higher Education, December 2000.